Pion axioproduction: The Δ resonance contribution

Thomas Vonk[*]

Helmholtz-Institut für Strahlen- und Kernphysik and Bethe Center for Theoretical Physics,
Universität Bonn, D-53115 Bonn, Germany

Feng-Kun Guo[†]

CAS Key Laboratory of Theoretical Physics, Institute of Theoretical Physics,
Chinese Academy of Sciences, Beijing 100190, China
and School of Physical Sciences, University of Chinese Academy of Sciences, Beijing 100049, China

Ulf-G. Meißner[‡]

Helmholtz-Institut für Strahlen- und Kernphysik and Bethe Center for Theoretical Physics,
Universität Bonn, D-53115 Bonn, Germany,
Institute for Advanced Simulation, Institut für Kernphysik and Jülich Center for Hadron Physics,
Forschungszentrum Jülich, D-52425 Jülich, Germany and Tbilisi State University, 0186 Tbilisi, Georgia

The process of pion axioproduction, $aN \to \pi N$, with an intermediate Δ resonance is analyzed using baryon chiral parturbation theory. The Δ resonance is included in two ways: First, deriving the $a\Delta N$-vertices, the axion is brought into contact with the resonance, and, second, taking the results of πN elastic scattering including the Δ, it is implicitly included in the form of a pion rescattering diagram. As a result, the partial wave cross section of axion-nucleon scattering shows an enhancement in the energy region around the Δ resonance. Because of the isospin breaking, the enhancement is not as pronounced as previously anticipated. However, since the isospin breaking here is much milder than that for usual hadronic processes, novel axion-search experiments might still exploit this effect.

I. INTRODUCTION

A model that might resolve two of the known problems of two different (but related) physical fields—in the present case the strong-CP problem of quantum chromodynamics (QCD) and the dark matter issue of astrophysics and cosmology [1–7]—is clearly worth investigating. Such a model is the Peccei-Quinn model [8,9] and the theory of the axion [10,11], especially the "invisble" axion models such as the Kim-Shifman-Vainstein-Zakharov (KSVZ) axion model [12,13] and the Dine-Fischler-Srednicki-Zhitnitsky (DFSZ) axion model [14,15]. However, the time theorists and experimentalists effortfully spent on the search for signals that might verify this model now comprises more than four decades, and still there is no axion in sight.

Because of that it is important to study all kinds of related processes hoping to figure out some underlying phenomenon that might enhance the chance of its detection, if only for a few percent.

Recently, Carenza *et al.* [16] have proposed that the pion axioproduction [17] $aN \to \pi N$ is such a process, because at certain axion energies, around 200 MeV–300 MeV, an enhanced axion-nucleon cross section due to the Δ resonance can be expected. This in turn would possibly make axion detections accessible for underground water Cherenkov detectors. Such axions might be produced in protosupernova cores in the presence of pions, where besides the axion production via axion-nucleon bremsstrahlung $NN \to aNN$, the pion-induced process $\pi N \to aN$ might play a more important role than previously thought [16,18], leading to a possible enhancement of the number spectrum of axions with energies around 200 MeV–300 MeV.

In this study, we take a closer look at exactly this process, namely $aN \to \pi N$ with the Δ resonance, showing that there is indeed a region of enhancement. This enhancement is, however, at least an order of magnitude less pronounced than that anticipated by Carenza *et al.* [16], which we will discuss in more detail below in Sec. IV.

[*]vonk@hiskp.uni-bonn.de
[†]fkguo@itp.ac.cn
[‡]meissner@hiskp.uni-bonn.de

Having said that, it is important to remind the reader that the traditional window for the QCD axion as a dark matter candidate dictates [1,2,19,20]

$$10^9 \text{ GeV} \lesssim f_a \lesssim 10^{12} \text{ GeV}, \quad (1)$$

where f_a is the axion decay constant which eventually controls and suppresses the axion mass [21,22]

$$m_a \approx 5.7 \left(\frac{10^{12} \text{ GeV}}{f_a} \right) \times 10^{-6} \text{ eV}, \quad (2)$$

and the axion-nucleon coupling $G_{aN} \propto 1/f_a$. This means that despite the possible enhancement due to the presence of baryon resonances, the reaction cross section still remains tiny.

A very suitable framework for studying the process at hand is chiral perturbation theory (CHPT), which has been successfully extended to the meson-nucleon and Δ-meson-nucleon sectors, and which in the past also has been applied to the study of the axion-nucleon interaction [23,24], after the leading order axion-nucleon interaction had been studied for years in the context of current algebra, which is equivalent to a leading-order calculation in CHPT [25–29]. In this paper we use these results including the thereby accrued knowledge of the underlying structure of the axion-nucleon coupling. Moreover, we show how to include the Δ baryon into the model.

In Sec. II we first give a short discussion of the kinematics and the general isospin structure of the $aN \to \pi N$ scattering amplitude, as well as a brief presentation of baryon CHPT with axions and the Δ resonance. Then we work out the amplitudes of the individual Feynman diagrams contributing to the pion axioproduction in Sec. III. Putting the pieces together, we finally discuss the results in Sec. IV.

II. THEORETICAL FOUNDATION

A. Kinematics

The process under consideration is

$$a(q) + N(p) \to \pi^b(q') + N(p'), \quad (3)$$

where a denotes the axion, N is a nucleon (either the proton or the neutron), and π^b is a pion with the isospin index b. As usual, we define the Lorentz-invariant Mandelstam variables

$$s = (p+q)^2, \quad t = (p-p')^2, \quad u = (p-q')^2, \quad (4)$$

for the four-momenta q, p of the incoming particles and q', p' of the outgoing particles. The invariants of Eq. (4) fulfill the on shell relation

$$s + t + u = 2m_N^2 + m_a^2 + M_\pi^2, \quad (5)$$

which can be used to eliminate one of the three variables, which we choose to be u. Throughout this paper we use the center-of-mass system (c.m.), where for the three-momenta $\mathbf{p} + \mathbf{q} = \mathbf{p}' + \mathbf{q}' = 0$. Using the well-known Källén function

$$\lambda(a, b, c) = a^2 + b^2 + c^2 - 2ab - 2ac - 2bc, \quad (6)$$

the c.m. energies of the incoming and outgoing nucleons can be written as

$$E_{\mathbf{p}} = \frac{s + m_N^2 - m_a^2}{2\sqrt{s}}, \qquad E_{\mathbf{p}'} = \frac{s + m_N^2 - M_\pi^2}{2\sqrt{s}}, \quad (7)$$

and one has

$$|\mathbf{p}| = |\mathbf{q}| = \frac{\sqrt{\lambda(s, m_N^2, m_a^2)}}{2\sqrt{s}},$$

$$|\mathbf{p}'| = |\mathbf{q}'| = \frac{\sqrt{\lambda(s, m_N^2, M_\pi^2)}}{2\sqrt{s}}. \quad (8)$$

Moreover, setting $z = \cos\theta$, where θ is the c.m. scattering angle, we have

$$(\mathbf{p} \cdot \mathbf{p}') = |\mathbf{p}||\mathbf{p}'|z, \quad (9)$$

so we can reexpress the second Mandelstam t variable as

$$t = 2(m_N^2 - E_{\mathbf{p}}E_{\mathbf{p}'} + |\mathbf{p}||\mathbf{p}'|z). \quad (10)$$

Before discussing how these kinematic quantities enter the scattering amplitudes, we briefly take a look at the isospin structure of the process.

B. Isospin structure

For the πN elastic scattering, it is common to decompose the scattering amplitude $T_{\pi N \to \pi N}^{ab}$, where a is the isospin index of the incoming pion and b for the outgoing one, according to the isospin structure. In the isospin limit, the decomposition reads

$$T_{\pi N \to \pi N}^{ab} = T^+ \delta_{ab} + T^- \frac{1}{2}[\tau_a, \tau_b], \quad (11)$$

where τ_a and τ_b are the Pauli matrices and $[,]$ denotes the commutator. However, for the present process $aN \to \pi^b N$ we are particularly interested in transitions including the Δ resonance, as suggested in Ref. [16], which is an isospin-$\frac{3}{2}$ particle. As the axion is an isoscalar, no isospin symmetric aN interaction can lead to the appearance of the Δ resonance, so we are especially interested in isospin-breaking interactions. Indeed, the isovector axial-vector current a_μ (see below) introduces such isospin breaking pieces into the axion-baryon interaction, which can be seen, for instance, below in Eqs. (27) and (33).

As it turns out, it is possible to decompose the scattering amplitude $T_{aN \to \pi N}^b$ into

$$T_{aN\to\pi N}^b = T^+\delta_{3b} + T^{3+}\tau_3 + T^-\frac{1}{2}[\tau_b,\tau_3], \quad (12)$$

which is comparable to the case of πN scattering with isospin violation, see, e.g., Refs. [30,31]. Any of the four possible amplitudes can be expressed by means of the three objects T^+, T^{3+}, and T^-,

$$T_{ap\to\pi^0 p} = T^+ + T^{3+},$$
$$T_{an\to\pi^0 n} = T^+ - T^{3+},$$
$$T_{ap\to\pi^+ n} = \sqrt{2}(T^{3+} + T^-),$$
$$T_{an\to\pi^- p} = \sqrt{2}(T^{3+} - T^-). \quad (13)$$

The part of the amplitude that leads to isospin violation and thus to possible enhancement due to the Δ resonances, which we denote by $T^{3/2}$, is found by taking the difference

$$T^{3/2} = T^+ - T^-, \quad (14)$$

or alternatively,

$$T^{3/2} = T_{ap\to\pi^0 p} - \frac{1}{\sqrt{2}}T_{ap\to\pi^+ n}$$
$$= T_{an\to\pi^0 n} + \frac{1}{\sqrt{2}}T_{an\to\pi^- p}, \quad (15)$$

where the latter expressions have the advantage that one can also easily account for differences in the charged and neutral pion masses, which improves the accuracy of the calculation.

C. Partial wave decomposition

It is known from πN scattering that the Δ resonance chiefly affects the P_{33} partial wave (where we, as usual, make use of the spectroscopic notation $l_{2I,2j}$, $l = S, P, D, \dots$ being the orbital angular momentum, I being the isospin, and $j = l + s$ the total angular momentum). Therefore, it is expedient to also focus on the P_{33} partial wave in the present study of the $aN \to \pi N$ reaction.

To this end, we decompose any of the amplitudes given above as

$$T = \bar{u}(p')\left\{A(s,t) + B(s,t)\frac{1}{2}(\slashed{q}+\slashed{q}')\right\}u(p), \quad (16)$$

where we make use of the well-known notation, $\slashed{q} = \gamma^\mu q_\mu$. One then can project out any partial wave of definite total angular momentum $j = l \pm 1/2$, abbreviated as $l\pm$, by

$$T_{l\pm}(s) = \frac{\sqrt{E_\mathbf{p}+m_N}\sqrt{E_{\mathbf{p}'}+m_N}}{2}\{A_l(s)+(\sqrt{s}-m_N)B_l(s)\} + \frac{\sqrt{E_\mathbf{p}-m_N}\sqrt{E_{\mathbf{p}'}-m_N}}{2}\{-A_{l\pm1}(s)+(\sqrt{s}+m_N)B_{l\pm1}(s)\}, \quad (17)$$

where

$$A_l(s) = \int_{-1}^{+1}A(s,t(s,z))P_l(z)\mathrm{d}z,$$
$$B_l(s) = \int_{-1}^{+1}B(s,t(s,z))P_l(z)\mathrm{d}z, \quad (18)$$

using the well-known Legendre polynomials $P_l(z)$.

D. Partial wave cross section

For experiments, the most useful quantity is the cross section

$$\mathrm{d}\sigma = \frac{1}{\mathcal{F}}|\mathcal{M}|^2\mathrm{d}\Pi_2, \quad (19)$$

with the flux factor

$$\mathcal{F} = 4\sqrt{(p\cdot q)-m_N m_a} = 4|\mathbf{p}|\sqrt{s}, \quad (20)$$

and the two-body phase space

$$\int \mathrm{d}\Pi_2 = \int \frac{\mathrm{d}^3 p'}{(2\pi)^3}\frac{\mathrm{d}^3 q'}{(2\pi)^3}\frac{1}{2E_{\mathbf{p}'}2E_{\mathbf{q}'}}(2\pi)^4\delta^4(p+q-p'-q')$$
$$= \int \mathrm{d}\Omega\frac{1}{16\pi^2}\frac{|\mathbf{p}'|}{\sqrt{s}}, \quad (21)$$

where in both cases the right-most expressions are valid in the c.m. frame. The total cross section is hence given by

$$\sigma = \frac{1}{64\pi^2 s}\frac{|\mathbf{p}'|}{|\mathbf{p}|}\int \mathrm{d}\Omega|\mathcal{M}|^2, \quad (22)$$

which can be expanded in terms of partial wave cross sections as

$$\sigma = \sum_l \sigma_{l\pm}. \tag{23}$$

The inverse of Eq. (17) is given by

$$T = 2m_N \chi_f^\dagger \sum_l \left\{ [(l+1)T_{l+} + lT_{l-}]P_l(z) \right.$$
$$\left. - i\boldsymbol{\sigma} \cdot (\hat{\mathbf{q}}' \times \hat{\mathbf{q}})(T_{l+} - T_{l-})\frac{dP_l}{dz} \right\} \chi_i, \tag{24}$$

where χ_i and χ_f are the Pauli spinors of the incoming and outgoing nucleons, respectively, and $\hat{\mathbf{q}}^{(\prime)} = \mathbf{q}^{(\prime)}/|\mathbf{q}^{(\prime)}|$. For the $j = \frac{3}{2}$ case, one finds

$$\sigma_{1+} = \frac{1}{8\pi s}\frac{|\mathbf{p}'|}{|\mathbf{p}|}|T_{1+}|^2. \tag{25}$$

The bottom line of the previous elaborations then is that we will derive the amplitudes $A^{\pm,3+}(s,t)$ and $B^{\pm,3+}(s,t)$ for any Feynman diagram of interest and use Eqs. (12) and (17) in order to determine the P_{33} partial wave amplitude $T_{aN\to\pi N}^{33}$ for the pertinent processes. This amplitude in turn is used to ascertain the corresponding cross section via Eq. (25). The theoretical framework of determining $A^{\pm,3+}(s,t)$ and $B^{\pm,3+}(s,t)$ is CHPT.

E. Baryon chiral perturbation theory with axions

The way of incorporating the axion into CHPT is discussed in detail in Ref. [24]. Here, we will only outline the major steps. First, recall that in the standard QCD axion models, the KSVZ and DFSZ ones, the axion-quark couplings X_q appearing in the QCD Lagrangian after the spontaneous breakdown of Peccei-Quinn symmetry are flavor diagonal and given by

$$X_q^{\mathrm{KSVZ}} = 0,$$
$$X_{u,c,t}^{\mathrm{DFSZ}} = \frac{1}{3}\frac{x^{-1}}{x+x^{-1}} = \frac{1}{3}\sin^2\beta,$$
$$X_{d,s,b}^{\mathrm{DFSZ}} = \frac{1}{3}\frac{x}{x+x^{-1}} = \frac{1}{3}\cos^2\beta = \frac{1}{3} - X_{u,c,t}^{\mathrm{DFSZ}}, \tag{26}$$

where $x = \cot\beta$ is the ratio of the vacuum expectation values of the two Higgs doublets in the DFSZ model. After a chiral rotation removing the axion-gluon coupling terms in the Lagrangian, the whole axion-quark interaction can be decomposed into isovector and isoscalar parts with the couplings

$$c_{u-d} = \frac{1}{2}\left(X_u - X_d - \frac{1-z}{1+z+w}\right),$$
$$c_{u+d} = \frac{1}{2}\left(X_u + X_d - \frac{1+z}{1+z+w}\right),$$
$$c_s = X_s - \frac{w}{1+z+w},$$
$$c_{c,b,t} = X_{c,b,t}, \tag{27}$$

where $z = m_u/m_d$ and $w = m_u/m_s$ are the quark mass ratios of the three light quarks. In what follows, the c_i, $(i = \{1, \ldots, 5\})$, refer to the isoscalar couplings $\{u+d, s, c, b, t\}$ and in any equation a summation over repeated i is implied. It is these couplings that enter the Lagrangian of CHPT in the form of external currents [32]

$$a_\mu = c_{u-d}\frac{\partial_\mu a}{2f_a}\tau_3, \qquad a_{\mu,i}^{(s)} = c_i\frac{\partial_\mu a}{2f_a}\mathbb{1}. \tag{28}$$

The transition to CHPT is phenomenologically related to the confinement of quarks and gluons into mesons and baryons at low energies and the observation that the QCD Lagrangian is approximately invariant under the chiral symmetry $\mathrm{SU}(N_f)_L \times \mathrm{SU}(N_f)_R$, with N_f the number of light quark flavors, which is spontaneously broken into the vector subgroup. Hence, in SU(2) baryon CHPT nucleons and pions are the relevant degrees of freedom rather than the more fundamental quarks and gluons. The application of power counting rules then leads to a systematic perturbative description of any low-energy strong interaction process, as long as the applied Lagrangian respects all pertinent symmetries, as first worked out by Weinberg [33].

For the meson-nucleon sector that we are interested in, we follow the description of baryon CHPT given in Ref. [34]. The pions enter the theory in the form of a unitary 2×2 matrix

$$u = \sqrt{U} = \exp\left(i\frac{\pi^a\tau_a}{2F_\pi}\right), \tag{29}$$

where F_π is the pion decay constant. Strictly speaking, this should be the pion decay constant in the chiral limit, F, but to the order we are working on we can use the physical value. With this unitary matrix and the external currents a_μ and $a_\mu^{(s)}$, see Eq. (28), one forms the following basic building blocks

$$u_\mu = i[u^\dagger\partial_\mu u - u\partial_\mu u^\dagger - iu^\dagger a_\mu u - iua_\mu u^\dagger],$$
$$u_{\mu,i} = i[-iu^\dagger a_{\mu,i}^{(s)}u - iua_{\mu,i}^{(s)}u^\dagger] = 2a_{\mu,i}^{(s)},$$
$$D_\mu = \partial_\mu + \Gamma_\mu$$
$$= \partial_\mu + \frac{1}{2}[u^\dagger\partial_\mu u + u\partial_\mu u^\dagger - iu^\dagger a_\mu u + iua_\mu u^\dagger]. \tag{30}$$

Note that we only introduce and show the axial-vector currents a_μ (isovector) and $a_\mu^{(s)}$ (isoscalar) (and not the corresponding vector currents) as these are the only external currents that are of interest in what follows. The last object in Eq. (30), D_μ, is the so-called chiral covariant derivative. At leading order, the axion only enters the model via these building blocks. At higher order, it also enters in the form of nonderivative interactions by means of terms involving the complex phase of the quark mass matrix.

In what follows, we only need the leading order pion-nucleon Lagrangian, which is given by

$$\mathcal{L}_{\pi N} = \bar{N}\left\{ i\slashed{D} - m_N + \frac{g_A}{2}\slashed{a}\gamma_5 + \frac{g_0^i}{2}\slashed{a}_i\gamma_5 \right\}N, \quad (31)$$

where $N = (p, n)^{\mathrm{T}}$ is an isodoublet containing the proton and the neutron spinors, m_N is the nucleon mass in the chiral limit, and g_A and the g_0^i's are the axial-vector and corresponding isoscalar coupling constants, all also in the chiral limit. Again, to the order we are working, we can identify these parameters with their physical values.

In Ref. [24], we already worked out and used the relevant vertices that can be derived from this Lagrangian and which are also needed for the present study. Denoting the momentum of an incoming axion with q_μ and setting b as the pion isospin index, one finds for the relevant vertices,

$$aNN: \frac{g_{aN}}{2f_a}\slashed{q}\gamma_5,$$
$$a\pi_b NN: i\frac{c_{u-d}}{4f_a F_\pi}\slashed{q}[\tau_3, \tau_b]. \quad (32)$$

The latter contact interaction is often ignored in studies of the aN reaction, which are mainly based on the former vertex, but has recently been included in the study of axion production in supernovae [35].

The axion-nucleon coupling appearing in Eq. (32) is a 2×2 matrix in isospin space defined as

$$g_{aN} = c_{u-d}g_A\tau_3 + c_i g_0^i \mathbb{1}, \quad (33)$$

from which one can directly read off the couplings of the axion to the proton, g_{ap}, and the neutron, g_{an}, respectively.

F. The Δ resonance in chiral perturbation theory

The free-field Lagrangian of the four Δ baryons is given by [36–41]

$$\mathcal{L}_\Delta = \bar{\Delta}_\mu \Lambda^{\mu\nu}(A)\Delta_\nu, \quad (34)$$

where

$$\Delta_\mu = \begin{pmatrix} \Delta_\mu^{++} \\ \Delta_\mu^{+} \\ \Delta_\mu^{0} \\ \Delta_\mu^{-} \end{pmatrix} \quad (35)$$

is the spin-$\frac{3}{2}$ and isospin-$\frac{3}{2}$ vector-spinor field, and

$$\Lambda^{\mu\nu}(A = -1) = -(i\slashed{\partial} - m_\Delta) + i(\gamma^\mu\partial^\nu + \gamma^\nu\partial^\mu - \gamma^\mu\slashed{\partial}\gamma^\nu) - m_\Delta\gamma^\mu\gamma^\nu. \quad (36)$$

Here, m_Δ denotes the mass of the Δ and A is a nonphysical parameter that for convenience has been set to -1. The propagator for the Δ with four-momentum p^μ is then given by

$$-i\frac{\slashed{p} + m_\Delta}{p^2 - m_\Delta^2}\left[g^{\mu\nu} - \frac{1}{3}\gamma^\mu\gamma^\nu + \frac{1}{3m_\Delta}(p^\mu\gamma^\nu - \gamma^\mu p^\nu) - \frac{2}{3m_\Delta^2}p^\mu p^\nu \right]. \quad (37)$$

The $\pi N\Delta$ and the $aN\Delta$ interactions are derived from the general leading-order interaction Lagrangian given by [37,42]

$$\mathcal{L}_{\mathrm{int.}} = \frac{g}{2}\bar{\Delta}_{\mu,i}(g^{\mu\nu} + z_0\gamma^\mu\gamma^\nu)\langle\tau_i u_\nu\rangle N + \mathrm{H.c.}, \quad (38)$$

where H.c. stands for the Hermitian conjugate and $\langle\rangle$ denotes the trace in flavor space. Furthermore, we make use of the isospurion representation $\Delta_{\mu,i} = \mathcal{T}_i\Delta_\mu$ with the 2×4 isospin-$\frac{1}{2}$-to-isospin-$\frac{3}{2}$ transition matrices [37,43]

$$\mathcal{T}_1 = \frac{1}{\sqrt{6}}\begin{pmatrix} -\sqrt{3} & 0 & 1 & 0 \\ 0 & -1 & 0 & \sqrt{3} \end{pmatrix},$$
$$\mathcal{T}_2 = \frac{-i}{\sqrt{6}}\begin{pmatrix} \sqrt{3} & 0 & 1 & 0 \\ 0 & 1 & 0 & \sqrt{3} \end{pmatrix},$$
$$\mathcal{T}_3 = \sqrt{\frac{2}{3}}\begin{pmatrix} 0 & 1 & 0 & 0 \\ 0 & 0 & 1 & 0 \end{pmatrix}, \quad (39)$$

such that

$$\Delta_{\mu,1} = \frac{1}{\sqrt{2}}\begin{pmatrix} \frac{1}{\sqrt{3}}\Delta_\mu^0 - \Delta_\mu^{++} \\ \Delta_\mu^- - \frac{1}{\sqrt{3}}\Delta_\mu^+ \end{pmatrix},$$
$$\Delta_{\mu,2} = -\frac{i}{\sqrt{2}}\begin{pmatrix} \frac{1}{\sqrt{3}}\Delta_\mu^0 + \Delta_\mu^{++} \\ \Delta_\mu^- + \frac{1}{\sqrt{3}}\Delta_\mu^+ \end{pmatrix},$$
$$\Delta_{\mu,3} = \sqrt{\frac{2}{3}}\begin{pmatrix} \Delta_\mu^+ \\ \Delta_\mu^0 \end{pmatrix}. \quad (40)$$
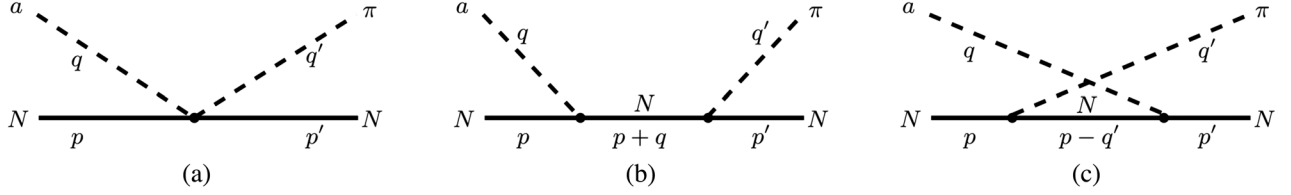
FIG. 1. Tree-level contributions to $aN \to \pi N$ without the Δ intermediate state. (a) contact interaction, (b) s channel, and (c) crossed channel.

The interaction Lagrangian Eq. (38) contains two coupling constants g and z_0, the latter being an off shell parameter. N again denotes the nucleon doublet and u_μ has been given already above in Eq. (30). Note that this interaction Lagrangian only allows for isovector interactions with external axial currents a_μ, whereas isoscalar interactions with $a_{\mu,i}^{(s)}$ vanish as a consequence of the trace operation. This reflects what has been said already above; any $aN\Delta$ interaction must come with isospin violation, which is only present in a_μ, not in $a_{\mu,i}^{(s)}$.

III. RELEVANT DIAGRAMS AND THEIR CONTRIBUTIONS

A. Contact contribution and intermediate nucleon

Having set up the kinematic environment and the theoretical framework, we can now explore several contributions to the $aN \to \pi N$ scattering amplitude. We start with the tree-level contact and Born graphs shown in Fig. 1. The results can be obtained in a rather straightforward fashion by using the vertices of Eq. (32) and the πN vertex of the Lagrangian Eq. (31).

The contact interaction, Fig. 1(a), only gives a contribution to B^- and is free of any kinematic variable,

$$B_{1a}^- = \frac{c_{u-d}}{2 f_a F_\pi}. \tag{41}$$

This means that the contact interaction is solely present in the $ap \to \pi^+ n$ and $an \to \pi^- p$ processes, but absent in any process involving the neutral pion. For the diagrams of Figs. 1(b) and 1(c), one gets

$$A_{1b,1c}^+ = \frac{g_A^2 c_{u-d} m_N}{f_a F_\pi},$$

$$B_{1b,1c}^+(s,t) = -\frac{g_A^2 c_{u-d} m_N^2}{f_a F_\pi}\left(\frac{1}{s-m_N^2} - \frac{1}{u-m_N^2}\right),$$

$$A_{1b,1c}^{3+} = \frac{g_A g_0^i c_i m_N}{f_a F_\pi},$$

$$B_{1b,1c}^{3+}(s,t) = -\frac{g_A g_0^i c_i m_N^2}{f_a F_\pi}\left(\frac{1}{s-m_N^2} - \frac{1}{u-m_N^2}\right),$$

$$A_{1b,1c}^- = 0,$$

$$B_{1b,1c}^-(s,t) = -\frac{g_A^2 c_{u-d} m_N}{2 f_a F_\pi}\left[1 + 2m_N\left(\frac{1}{s-m_N^2} + \frac{1}{u-m_N^2}\right)\right], \tag{42}$$

where u needs to be understood as $u(s,t)$ via Eq. (5). In the Appendix, we give a different expression of these contributions in terms of the axion-nucleon coupling constants g_{an} and g_{ap} for each of the four possible $aN \to \pi N$ channels. However, for the study of the P_{33} partial wave, it is not expedient to rewrite them in terms of g_{an} and g_{ap}, because after forming the difference Eq. (14), one can nicely see that the isoscalar terms $\propto c_i$ stemming from $a_{\mu,i}^{(s)}$ drop out, leaving only the isospin violating portion $\propto c_{u-d}$ that originates from a_μ. This fact makes it easy to show (as will be done below) that in the case of the P_{33} partial wave the KSVZ axion can be treated as a special case of the DSFZ axion.

B. Intermediate Δ resonance

Including the Δ leads to the diagrams shown in Fig. 2. As the two diagrams are related by crossing, it is convenient to define

$$A_\Delta(s,t) = \frac{2g^2 c_{u-d}}{3 f_a F_\pi}\left\{\frac{2z_0}{3m_\Delta^2}[m_\Delta + (m_N + 2m_\Delta)z_0](s - m_N^2) + \frac{1}{s - \mu_\Delta^2}\left[(m_N + m_\Delta)\left(\frac{1}{2}[m_a^2 + M_\pi^2 - t] - \frac{1}{3}[s - m_N^2]\right)\right.\right.$$

$$\left.\left. - \frac{1}{6m_\Delta^2}\left((m_N + m_\Delta)([m_a^2 + M_\pi^2][s - m_N^2] + m_a^2 M_\pi^2) + m_a^2 M_\pi^2 m_\Delta + m_N(s - m_N^2)^2\right)\right]\right\}, \tag{43}$$

and
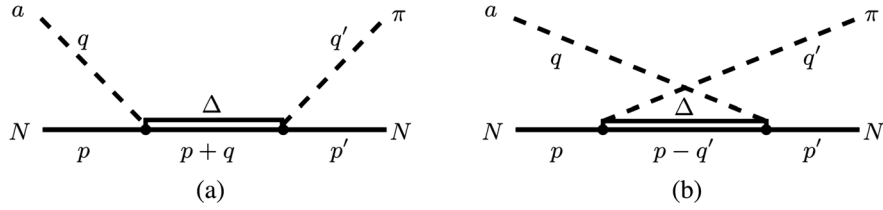
FIG. 2.   Tree-level contributions to $aN \to \pi N$ with an intermediate Δ state. (a) s channel and (b) crossed channel.

$$B_\Delta(s,t) = \frac{2g^2 c_{u-d}}{3f_a F_\pi} \left\{ -\frac{z_0}{3m_\Delta^2} \left[m_a^2 + M_\pi^2 + 2(s - m_N^2)(1 + z_0) + 4m_N m_\Delta(1 + z_0) + 4m_N(m_N + m_\Delta)z_0 \right] \right.$$
$$+ \frac{1}{s - \mu_\Delta^2} \left[\frac{1}{2}[m_a^2 + M_\pi^2 - t] - \frac{1}{6}m_a^2 + \frac{1}{6m_\Delta}(m_N + m_\Delta)(4m_N m_\Delta - M_\pi^2) \right.$$
$$\left. \left. - \frac{1}{6m_\Delta^2}[(m_a^2 + M_\pi^2 + 2m_N m_\Delta)(s - m_N^2) + m_a^2(m_N m_\Delta + M_\pi^2) + (s - m_N^2)^2] \right] \right\}. \tag{44}$$

Here the axion mass terms are kept explicitly though they, being tiny for the standard QCD axion models, can be safely neglected.

Then one can combine both diagrams and obtains the following expressions

$$A_\Delta^+(s,t) = A_\Delta(s,t) + A_\Delta(u,t),$$
$$B_\Delta^+(s,t) = B_\Delta(s,t) - B_\Delta(u,t),$$
$$A_\Delta^-(s,t) = -\frac{1}{2}[A_\Delta(s,t) - A_\Delta(u,t)],$$
$$B_\Delta^-(s,t) = -\frac{1}{2}[B_\Delta(s,t) + B_\Delta(u,t)], \tag{45}$$

where again $u = u(s,t)$. Note that there is no contribution to T^{3+}. Equations (43) and (44) have a pole appearing at c.m. energies around the Δ mass squared. In order to circumvent any unnecessary subtleties related to this, we use a Breit-Wigner propagator with a complex mass squared

$$\mu_\Delta^2 = m_\Delta^2 - i m_\Delta \Gamma_\Delta \tag{46}$$

with $m_\Delta \approx 1232$ MeV and $\Gamma_\Delta \approx 117$ MeV the Breit-Wigner mass and width of the Δ resonance. A more refined treatment could e.g., be given by including the Δ self-energy in the complex mass scheme, but that is not required here.

C. Pion rescattering

Another sort of diagram that contributes is shown in Fig. 3. As in the previous diagrams, the left (smaller) vertex leads to an axion-pion conversion (so this vertex basically comprises the contributions of Fig. 1). This pion consequently gets rescattered in the ordinary πN scattering. The latter (larger) vertex treated in a proper way also includes contributions from the Δ baryon. As this is an often studied process, we can base the treatment of this diagram on previous results. In particular, we will adopt the method and results of Refs. [44,45].

The diagrams that contribute to the πN scattering at this order are basically the same as the ones discussed in the previous subsections, but with the axion replaced by another pion. Using Eqs. (11) and (17) leads to a projection to the P_{33} partial wave. We do not repeat the results for the diagrams here, they can be found in Ref. [44], Eqs. (3.4) and (3.9) [46]. Moreover, we also adopt the results for the renormalized chiral pion loops obtained in heavy baryon CHPT (HBCHPT) from [47] (which are needed for the unitarization, see below).

As the πN scattering above threshold and below the appearance of inelastic reactions fulfills the unitarity relation (here $W = \sqrt{s}$, the c.m. energy)

$$\text{Im} T_{l\pm}^I(W) = \frac{|\mathbf{q}|}{8\pi W}|T_{l\pm}^I(W)|^2, \tag{47}$$

the pole in the Δ propagator can be treated in a more systematic way than the one we used in Sec. III B for the $aN \to \pi N$ reaction. In particular, a suitable unitarization technique can be used to restore unitarity which is otherwise only fulfilled perturbatively in CHPT. The method used in Ref. [44] is the N/D method [48,49]. In a nutshell,
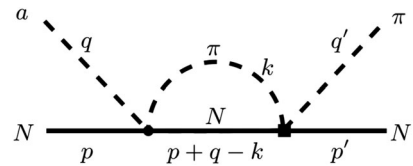
FIG. 3.   The pion-rescattering diagram for $aN \to \pi N$.

it is based on the observation that the unitarity relation leads to a right-hand cut in the partial wave T-matrix such that one can write down a dispersion relation for the inverse amplitude with some extra terms which are free of any right-hand cuts. These can be matched to the amplitudes obtained from CHPT. This effectively corresponds to a resummation of the relevant diagrams. Possible double counting can be avoided by the matching procedure discussed in Ref. [45]. The integral of the dispersion relation can be performed analytically and is basically given by the known two-point loop function involving one pion and one nucleon,

$$g(s) = \frac{1}{16\pi^2} \left\{ a_0(\mu) + \left(1 - \frac{w}{m_N} \right) \log \left(\frac{M_\pi^2}{\mu^2} \right) \right. $$
$$\left. - x_+ \log \left(\frac{x_+ - 1}{x_+} \right) - x_- \log \left(\frac{x_- - 1}{x_-} \right) \right\}, \quad (48)$$

at a renormalization scale μ. We take μ as the nucleon mass, and any change in μ can be reabsorbed by the subtraction constant $a_0(\mu)$. Furthermore, w is the c.m. pion energy and

$$x_\pm = \frac{s + m_N^2 - M_\pi^2}{2s} \pm \frac{1}{2s} \sqrt{\lambda(s, m_N^2, M_\pi^2)}. \quad (49)$$

The matching procedure for unitarizing the leading one-loop $\mathcal{O}(p^3)$ amplitude with the Δ resonance leads to

$$T_{\pi N}^{I,l\pm}$$
$$= \frac{1}{\left(T_{\text{tree}}^{I,l\pm} + T_{\text{loop}}^{I,l\pm} + T_\Delta^{I,l\pm} + \frac{2\sqrt{s}}{E_{\mathbf{p}} + m_N} (T_{\text{LO}}^{I,l\pm})^2 g(s) \right)^{-1} + g(s)},$$
$$(50)$$

which indeed fulfills Eq. (47). Note that the tree contributions $T_{\text{tree}}^{I,l\pm}$ and $T_\Delta^{I,l\pm}$ for the resonance are taken as being the full relativistic ones, whereas $T_{\text{LO}}^{I,l\pm}$ is only the very leading-order HBCHPT amplitude.

Returning to pion axioproduction, we performed a full reanalysis of the phase shift $\delta_{l\pm}^I$ defined by

$$T_{l\pm}^I(W) = \frac{8\pi W}{|\mathbf{q}|} \exp(i\delta_{l\pm}^I) \sin(\delta_{l\pm}^I) \quad (51)$$

in order to use these results for the rescattering diagram and in order to determine accurate values for the coupling constants g and z_0 of Eq. (38) and a_0 of Eq. (48). The latter goal is achieved by fitting the resulting P_{33} phase shift to the results of the Roy-Steiner analysis of the πN scattering [50]. As input values we used the isospin-averaged nucleon mass $m_N = (m_n + m_p)/2 = 938.92$ MeV, the isospin-averaged pion mass $M_\pi = 138.03$ MeV, $F_\pi = 92.4$ MeV, and $m_\Delta = 1232$ MeV. The value of g_A is given below in
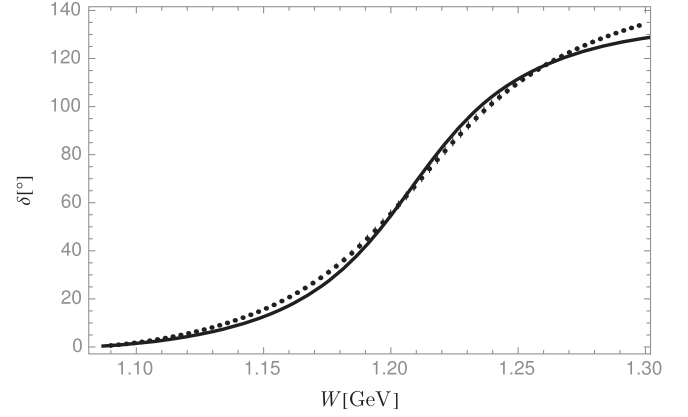
FIG. 4. The πN phase shift δ in the P_{33} channel (solid line) fitted to the results of the Roy-Steiner analysis (dots) from [50].

Sec. IV where we discuss the determination of the axion-baryon couplings, see Eq. (55). The fit to the phase shift values at $W \lesssim 1.3$ GeV yields

$$g = 1.249(16), \quad z_0 = -0.21(56), \quad a_0 = -0.959(12), \quad (52)$$

and is shown in Fig. 4.

Finally, the rescattering diagram is evaluated by

$$T_{\text{rescatt.}}^{33}(s) = \left(T_{ap \to \pi^0 p}^{33,\text{tree}}(s) g(s, M_{\pi^0}) \right.$$
$$\left. - \frac{1}{\sqrt{2}} T_{ap \to \pi^+ n}^{33,\text{tree}}(s) g(s, M_{\pi^+}) \right) T_{\pi N}^{33}(s), \quad (53)$$

where $g(s, M_{\pi^{+,0}})$ is the pion-nucleon loop function Eq. (48) with the meson (nucleon) mass being the charged and neutral pion (neutron and proton) mass, respectively. $T_{aN \to \pi N}^{33,\text{tree}}$ denotes the partial wave projected amplitudes of Sec. III A and $T_{\pi N}^{33}$ the unitarized P_{33} partial wave amplitude just discussed. We consider the usage of the latter appropriate even though it is derived using on shell kinematics, as the off shell effects are certainly subleading [51].

The expression in the parentheses is the proper way of getting the isospin violating part of the amplitude, as discussed in Sec. II B, see Eq. (15), i.e., by taking the difference of the amplitudes and the difference in the charged and neutral pion/nucleon masses. If one neglects this mass difference, one might as well use Eq. (14) instead yielding

$$T_{\text{rescatt.}}^{33}(s) = T_{aN \to \pi N}^{33,\text{tree}}(s) g(s, M_\pi) T_{\pi N}^{33}(s), \quad (54)$$

where $T_{aN \to \pi N}^{33,\text{tree}}$ now is the $j = \frac{3}{2}$ projection of $T^{I=3/2}$, Eq. (14), and M_π is the isospin-averaged pion mass. In fact, this latter approximation gives an average deviation of only $\lesssim 2\%$ in comparison to Eq. (53), which is valid for the KSVZ axion and the DFSZ axion at $\sin^2 \beta \lesssim 0.95$. Only for

values $\sin^2\beta \to 1$ the deviation becomes more pronounced at c.m. energies $W \gtrsim 1.15$ GeV reaching a maximum of about 15%. This means that Eq. (54) is a very good approximation for the vast majority of cases.

IV. RESULTS

Let us take the last result of the previous section as a starting point for the discussion of the overall results of this study. If one indeed takes the approximation of equal pion/nucleon masses, then Eq. (12) causes that any dependence on the isoscalar couplings $g_0^i c_i$ is canceled and any dependence on the axion-nucleon coupling g_{aN} in this process reduces to a dependence on $g_A c_{u-d}$ only, which reflects that this part of the coupling enforces the isospin violation needed to enable the Δ resonance appearance. For the same reason, the diagrams of Fig. 2 with the explicit Δ solely depend on c_{u-d} and not on the c_i's. This has two consequences: First, the total amplitude for the DFSZ axion with $\sin^2\beta$ in the interval [0, 1] and that for the KSVZ model will be $\propto c_{u-d}$; they have entirely the same shape, and only the magnitude changes as $\sin^2\beta$ is varied. Second, as c_{u-d} only depends on the difference $X_u - X_d$, one can easily determine a value for $\sin^2\beta$ such that $c_{u-d}^{\mathrm{DFSZ}}(\sin^2\beta) = c_{u-d}^{\mathrm{KSVZ}}$, which is accomplished when $\sin^2\beta = \frac{1}{2}$ [see Eq. (26)]. The $aN \to \pi N$ scattering amplitude in the P_{33} channel for the KSVZ axion is hence exactly the same as that for the DFSZ axion at $\sin^2\beta = \frac{1}{2}$. As the deviation from this approximation is only $\lesssim 2\%$, this remains basically true even if one considers Eq. (53) instead of Eq. (54).

For the calculation of the final scattering amplitude, we make use of the nucleon matrix elements in order to determine the isovector and isoscalar axial-vector couplings

$$g_A = \Delta u - \Delta d,$$
$$g_0^{u+d} = \Delta u + \Delta d,$$
$$g_0^q = \Delta q, \quad \text{for } q = s, c, b, t, \qquad (55)$$

where $s^\mu \Delta q = \langle p|\bar{q}\gamma^\mu\gamma_5 q|p\rangle$, with s^μ the spin of the proton. Of course, for the approximation discussed in the previous paragraph, only the value of g_A is of interest. For these matrix elements and z and w appearing in Eq. (26), we take the recent values from Ref. [52],

$$\Delta u = 0.847(50),$$
$$\Delta d = -0.407(34),$$
$$\Delta s = -0.035(13),$$
$$z = 0.485(19),$$
$$w = 0.025(1), \qquad (56)$$

and ignore Δq for $q = c, b, t$.

In Fig. 5, we show the partial wave cross sections $\sigma_{aN \to \pi N}^{33}$ consisting of all the contributions discussed in Sec. III, for both with the approximation Eq. (54) and without it. Actually, the cross sections are multiplied by the factor f_a^2 in order to get rid of the unknown prefactor $1/f_a^2$. This unknown quantity also appears implicitly in the terms containing the axion mass in Eqs. (43) and (44), but has practically no effect as the axion mass $\propto 1/f_a$ can safely be neglected for the typical QCD axion window [Eq. (1)]. However, this prefactor has to be kept in mind when considering the strength of the amplitudes in Fig. 5.

As anticipated, the curves for different values of $\sin^2\beta$ are identical up to the order of magnitude. As the absolute value of c_{u-d} is a linearly-decreasing function of $\sin^2\beta$, the magnitude steadily decreases, which makes a DFSZ axion with $\sin^2\beta \to 1$ the most unfavorable candidate for detection. As expected from the description at the end of the previous section, there is almost no visual deviation of the curves with approximation Eq. (54) and without it. Only for $\sin^2\beta = 1$ this deviation becomes recognizable but is still a minor effect. Note that the figures for the limit values of $\sin^2\beta = \{0, 1\}$ are given rather for illustrative purposes, as in realistic DFSZ models perturbative constraints from the heavy quark Yukawa couplings yield an allowed range [0.25, 170] for $\cot\beta$ [22] corresponding to approximately $\sin^2\beta \in [0.00, 0.94]$.

As a result, there is indeed a considerable enhancement of the P_{33} partial wave cross section in the region of the Δ resonance, but this enhancement is considerably weaker than previously assumed by Carenza et al. [16], who estimated the cross section via $f_a^2 \sigma_{aN \to \pi N} \approx F_\pi^2 \sigma_{\pi N \to \pi N}$ taking a value of 100 mb for $\sigma_{\pi N \to \pi N}$ [53]. This estimation suggests a peak value $f_a^2 \sigma_{aN \to \pi N} \approx 1$ mb GeV^2. The discrepancy between the results of Fig. 5 and such estimation can be explained by the fact that $aN \to \pi N$ in the Δ sector is primarily an isospin breaking process, which always comes with an extra suppression. It is worthwhile to notice that the suppression of the isospin breaking here, characterized by the factor $(1 - z)/(1 + z) = (m_d - m_u)/(m_d + m_u) \approx 0.34$ for the model-independent part of c_{u-d} [see Eq. (27)], is much milder than that for usual isospin breaking in hadronic processes, characterized by $(m_d - m_u)/m_s$ or $(m_d - m_u)/\Lambda_{\mathrm{QCD}}$. Thus, the results given in Ref. [16] are to be multiplied by a factor 10^{-1} to 10^{-5}, depending on the value of the model-dependent factor $\sin^2\beta$, that is a suppression by at least one order of magnitude. Then the number of pions produced via $aN \to \pi N$ through the Δ resonance in a megaton water Cherenkov detector will be at most $\mathcal{O}(100)$ using the axion luminosity estimated in Ref. [16] for axions emitted from a supernova at 1 kiloparsec.

V. SUMMARY

In this study we presented an analysis of the pion axioproduction $aN \to \pi N$ with an intermediate Δ
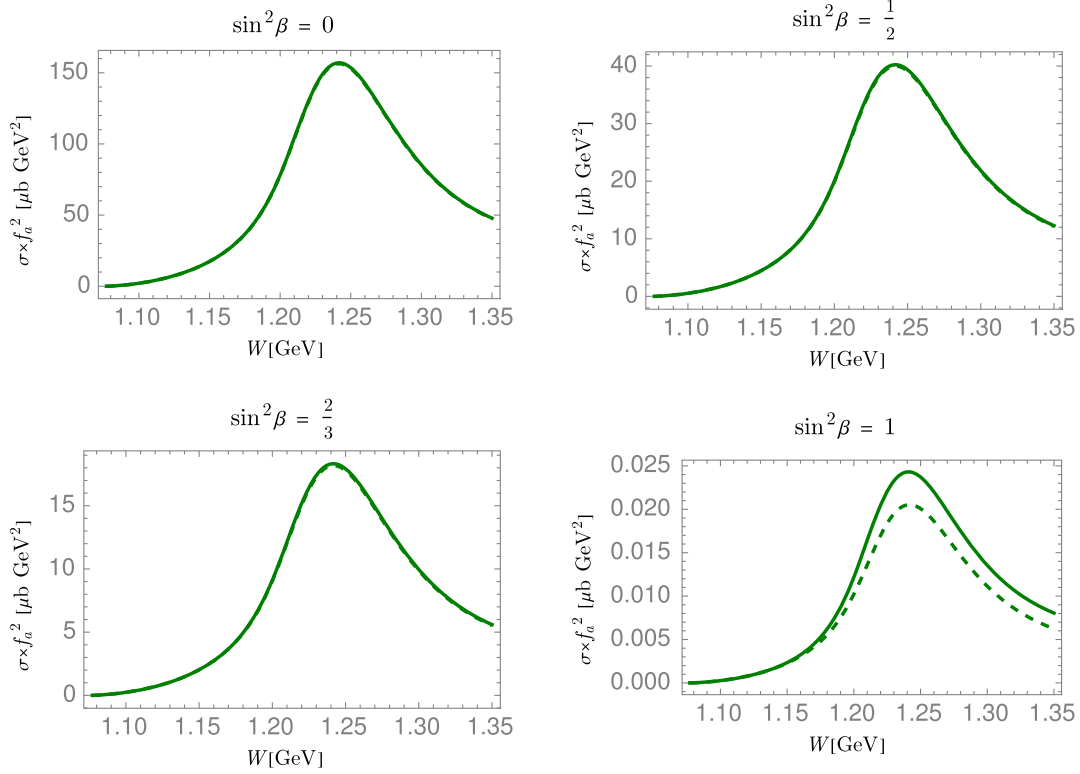
FIG. 5.　The $aN \to \pi N$ partial wave cross section of the P_{33} channel versus the c.m. energy W for the DFSZ axion at different values of $\sin^2 \beta$ and the KSVZ axion (which corresponds to $\sin^2 \beta = \frac{1}{2}$, see main text). The dashed curve corresponds to the approximated case based on Eq. (54).

resonance. We included the Δ resonance in two different ways: First, we used the chiral interaction Lagrangian for the Δ to bring the axion explicitly into contact with the resonance, and, second, we used the well-known results of πN elastic scattering with Δ to include it implicitly in the form of the rescattering diagram in Fig. 3.

As the Δ is a spin-$\frac{3}{2}$ and isospin-$\frac{3}{2}$ particle, it shows its full leverage effect in the P_{33} partial wave, which is why we concentrated on a study of this particular partial wave. For the same reason, this interaction is essentially an isospin violating process, as the axion is an isosinglet. We have shown that an approximation that concentrates on this isospin violation and that neglects any isoscalar coupling, while at the same time ignoring the pion and nucleon isospin mass splittings, is still very accurate unless $\sin^2 \beta$ approaches 1 in the DFSZ axion model (where it still gives quite good results). In this way, it is shown that the partial wave amplitude for the KSVZ axion equals that for the DFSZ axion at $\sin^2 \beta = \frac{1}{2}$.

Finally, the enhancement of the amplitude anticipated by Carenza *et al.* [16] is indeed present in the region of the Δ resonance, although it is considerably weaker than their naive estimation by at least an order of magnitude. This is basically a consequence of the isospin breaking suppression which is much milder than that for usual isospin breaking hadronic processes. Therefore, it might be

interesting to check whether other isospin-1/2 resonances such as the $N^*(1440)$ Roper resonance would provide an additional enhancement of the $aN \to \pi N$ cross section, as it is accessible without isospin breaking. The next step would hence be to investigate the impact of such resonances on the $aN \to \pi N$ reaction and consequently on the axion production in stellar objects, and whether this might be exploited to give fresh perspectives on experimental axion searches.

ACKNOWLEDGMENTS

APPENDIX: AMPLITUDES OF THE LEADING-ORDER TREE GRAPHS

In this appendix we give the full expression of the leading-order tree graph amplitudes of the four $aN \to \pi N$ channels. Using the abbreviation

$$R_\mu = \frac{1}{2}(q_\mu + q'_\mu), \tag{A1}$$

the contact contribution reads

$$T^{1a}_{aN \to \pi^0 N} = 0, \tag{A2}$$

$$T^{1a}_{ap \to \pi^+ n} = \frac{c_{u-d}}{\sqrt{2} f_a F_\pi} \bar{u}(p') \slashed{R} u(p), \tag{A3}$$

$$T^{1a}_{an \to \pi^- p} = -\frac{c_{u-d}}{\sqrt{2} f_a F_\pi} \bar{u}(p') \slashed{R} u(p), \tag{A4}$$

where the superscript refers to Fig. 1. For the other two diagrams Figs. 1(b) and 1(c) one gets

$$T^{1b,1c}_{ap \to \pi^0 p} = \frac{g_A m_N g_{ap}}{f_a F_\pi} \bar{u}(p') \left\{ 1 - m_N \left(\frac{1}{s - m_N^2} - \frac{1}{u - m_N^2} \right) \slashed{R} \right\} u(p), \tag{A5}$$

$$T^{1b,1c}_{an \to \pi^0 n} = -\frac{g_A m_N g_{an}}{f_a F_\pi} \bar{u}(p') \left\{ 1 - m_N \left(\frac{1}{s - m_N^2} - \frac{1}{u - m_N^2} \right) \slashed{R} \right\} u(p), \tag{A6}$$

$$T^{1b,1c}_{ap \to \pi^+ n} = \frac{g_A}{\sqrt{2} f_a F_\pi} \bar{u}(p') \left\{ 2 m_N g_0^i c_i - \left[g_A c_{u-d} + 2 m_N^2 \left(\frac{g_{ap}}{s - m_N^2} - \frac{g_{an}}{u - m_N^2} \right) \right] \slashed{R} \right\} u(p), \tag{A7}$$

$$T^{1b,1c}_{an \to \pi^- p} = \frac{g_A}{\sqrt{2} f_a F_\pi} \bar{u}(p') \left\{ 2 m_N g_0^i c_i + \left[g_A c_{u-d} - 2 m_N^2 \left(\frac{g_{an}}{s - m_N^2} - \frac{g_{ap}}{u - m_N^2} \right) \right] \slashed{R} \right\} u(p). \tag{A8}$$

Here, g_{an} and g_{ap} are the usual axion-nucleon couplings given in Eq. (33).

[1] J. Preskill, M. B. Wise, and F. Wilczek, Cosmology of the invisible axion, Phys. Lett. **120B,** 127 (1983).

[2] L. F. Abbott and P. Sikivie, A cosmological bound on the invisible axion, Phys. Lett. **120B,** 133 (1983).

[3] M. Dine and W. Fischler, The not so harmless axion, Phys. Lett. **120B,** 137 (1983).

[4] J. Ipser and P. Sikivie, Are Galactic Halos Made of Axions?, Phys. Rev. Lett. **50,** 925 (1983).

[5] M. S. Turner, Early-Universe Thermal Production of Not-So-Invisible Axions, Phys. Rev. Lett. **59,** 2489 (1987); Erratum, Phys. Rev. Lett.**60,** 1101(E) (1988).

[6] L. D. Duffy and K. van Bibber, Axions as dark matter particles, New J. Phys. **11,** 105008 (2009).

[7] D. J. E. Marsh, Axion cosmology, Phys. Rep. **643,** 1 (2016).

[8] R. D. Peccei and H. R. Quinn, Conservation in the Presence of Pseudoparticles, Phys. Rev. Lett. **38,** 1440 (1977).

[9] R. D. Peccei and H. R. Quinn, Constraints imposed by CP conservation in the presence of pseudoparticles, Phys. Rev. D **16,** 1791 (1977).

[10] S. Weinberg, A New Light Boson?, Phys. Rev. Lett. **40,** 223 (1978).

[11] F. Wilczek, Problem of Strong P and T Invariance in the Presence of Instantons, Phys. Rev. Lett. **40,** 279 (1978).

[12] J. E. Kim, Weak Interaction Singlet and Strong CP Invariance, Phys. Rev. Lett. **43,** 103 (1979).

[13] M. A. Shifman, A. I. Vainshtein, and V. I. Zakharov, Can confinement ensure natural CP invariance of strong interactions?, Nucl. Phys. **B166,** 493 (1980).

[14] M. Dine, W. Fischler, and M. Srednicki, A simple solution to the strong CP problem with a harmless axion, Phys. Lett. **104B,** 199 (1981).

[15] A. R. Zhitnitsky, On possible suppression of the axion hadron interactions. (In Russian), Sov. J. Nucl. Phys. **31,** 260 (1980).

[16] P. Carenza, B. Fore, M. Giannotti, A. Mirizzi, and S. Reddy, Enhanced Supernova Axion Emission and its Implications, Phys. Rev. Lett. **126,** 071102 (2021).

[17] We use the term axioproduction in analogy to terms like electroproduction or photoproduction. Pion axioproduction hence means pion production induced by axions.

[18] T. Fischer, P. Carenza, B. Fore, M. Giannotti, A. Mirizzi, and S. Reddy, Observable signatures of enhanced axion

emission from protoneutron stars, Phys. Rev. D **104,** 103012 (2021).

[19] J. E. Kim, Light pseudoscalars, particle physics and cosmology, Phys. Rep. **150,** 1 (1987).

[20] J. E. Kim and G. Carosi, Axions and the strong *CP* problem, Rev. Mod. Phys. **82,** 557 (2010); Erratum, Rev. Mod. Phys.**91,** 049902(E) (2019).

[21] Z.-Y. Lu, M.-L. Du, F.-K. Guo, U.-G. Meißner, and T. Vonk, QCD θ-vacuum energy and axion properties, J. High Energy Phys. 05 (2020) 001.

[22] L. Di Luzio, M. Giannotti, E. Nardi, and L. Visinelli, The landscape of QCD axion models, Phys. Rep. **870,** 1 (2020).

[23] G. Grilli di Cortona, E. Hardy, J. Pardo Vega, and G. Villadoro, The QCD axion, precisely, J. High Energy Phys. 01 (2016) 034.

[24] T. Vonk, F.-K. Guo, and U.-G. Meißner, Precision calculation of the axion-nucleon coupling in chiral perturbation theory, J. High Energy Phys. 03 (2020) 138.

[25] T. W. Donnelly, S. J. Freedman, R. S. Lytel, R. D. Peccei, and M. Schwartz, Do axions exist?, Phys. Rev. D **18,** 1607 (1978).

[26] D. B. Kaplan, Opening the axion window, Nucl. Phys. **B260,** 215 (1985).

[27] M. Srednicki, Axion couplings to matter. 1. *CP* conserving parts, Nucl. Phys. **B260,** 689 (1985).

[28] H. Georgi, D. B. Kaplan, and L. Randall, Manifesting the invisible axion at Low-energies, Phys. Lett. **169B,** 73 (1986).

[29] S. Chang and K. Choi, Hadronic axion window and the big bang nucleosynthesis, Phys. Lett. B **316,** 51 (1993).

[30] N. Fettes and U.-G. Meißner, Towards an understanding of isospin violation in pion nucleon scattering, Phys. Rev. C **63,** 045201 (2001).

[31] M. Hoferichter, B. Kubis, and U.-G. Meißner, Isospin violation in low-energy pion-nucleon scattering revisited, Nucl. Phys. **A833,** 18 (2010).

[32] Note the typo in Ref. [24], Eq. (3.16). $\tilde{u}_{\mu,i}$, which corresponds to $u_{\mu,i}$ in the present paper, is of course not $\propto \tau_3$, but $\propto \mathbb{1}$.

[33] S. Weinberg, Phenomenological lagrangians, Physica A (Amsterdam) **96A,** 327 (1979).

[34] V. Bernard, N. Kaiser, and U.-G. Meißner, Chiral dynamics in nucleons and nuclei, Int. J. Mod. Phys. E **04,** 193 (1995).

[35] K. Choi, H. J. Kim, H. Seong, and C. S. Shin, Axion emission from supernova with axion-pion-nucleon contact interaction, J. High Energy Phys. 02 (2022) 143.

[36] E. E. Jenkins and A. V. Manohar, Chiral corrections to the baryon axial currents, Phys. Lett. B **259,** 353 (1991).

[37] H.-B. Tang and P. J. Ellis, Redundance of Δ-isobar parameters in effective field theories, Phys. Lett. B **387,** 9 (1996).

[38] T. R. Hemmert, B. R. Holstein, and J. Kambor, Heavy baryon chiral perturbation theory with light deltas, J. Phys. G **24,** 1831 (1998).

[39] V. Pascalutsa and D. R. Phillips, Effective theory of the $\Delta(1232)$ resonance in Compton scattering off the nucleon, Phys. Rev. C **67,** 055202 (2003).

[40] C. Hacker, N. Wies, J. Gegelia, and S. Scherer, Including the Delta(1232) resonance in baryon chiral perturbation theory, Phys. Rev. C **72,** 055203 (2005).

[41] H. Krebs, E. Epelbaum, and U.-G. Meißner, On-shell consistency of the Rarita-Schwinger field formulation, Phys. Rev. C **80,** 028201 (2009).

[42] H. Krebs, E. Epelbaum, and U.-G. Meißner, Redundancy of the off-shell parameters in chiral effective field theory with explicit spin-3/2 degrees of freedom, Phys. Lett. B **683,** 222 (2010).

[43] V. Pascalutsa, M. Vanderhaeghen, and S. N. Yang, Electromagnetic excitation of the Delta(1232)-resonance, Phys. Rep. **437,** 125 (2007).

[44] U.-G. Meißner and J. A. Oller, Chiral unitary meson baryon dynamics in the presence of resonances: Elastic pion nucleon scattering, Nucl. Phys. **A673,** 311 (2000).

[45] J. A. Oller and U.-G. Meißner, Chiral dynamics in the presence of bound states: Kaon nucleon interactions revisited, Phys. Lett. B **500,** 263 (2001).

[46] As the diagrams of Fig. 2 and the corresponding diagrams of πN scattering are basically the same, the result of Ref. [44] can also be found by replacing $m_a \to M_\pi$ in Eqs. (43) and (44), adjusting of course the coupling constants in front.

[47] N. Fettes, U.-G. Meißner, and S. Steininger, Pion—nucleon scattering in chiral perturbation theory. 1. Isospin symmetric case, Nucl. Phys. **A640,** 199 (1998).

[48] G. F. Chew and S. Mandelstam, Theory of low-energy pion pion interactions, Phys. Rev. **119,** 467 (1960).

[49] J. A. Oller, Unitarization technics in hadron physics with historical remarks, Symmetry **12,** 1114 (2020).

[50] M. Hoferichter, J. Ruiz de Elvira, B. Kubis, and U.-G. Meißner, Roy–Steiner-equation analysis of pion–nucleon scattering, Phys. Rep. **625,** 1 (2016).

[51] M. Mai and U.-G. Meißner, New insights into antikaon-nucleon scattering and the structure of the Lambda(1405), Nucl. Phys. **A900,** 51 (2013).

[52] Y. Aoki *et al.,* FLAG review 2021, arXiv:2111.09849.

[53] The $\pi^+ p$ elastic cross section is the largest around the Δ resonance region, of about 100 mb [54].

[54] P. A. Zyla *et al.* (Particle Data Group), Review of particle physics, Prog. Theor. Exp. Phys. **2020,** 083C01 (2020).